CrossMark

Excellent Surface Enhanced Raman Scattering of SiO$_2$ Fiber Membrane Embedded with Ag Nanoparticles

Yuanzheng Tang[1,2] · Xiao Chen[1,2] · Yan Lv[1,2] · Zhengying Wu[1,2] · Feng Chen[1,2] · Zhigang Chen[1,2]

Abstract Uniformly distributed Ag nanoparticles supported on SiO$_2$ fiber membrane materials were successfully synthesized using electrospinning and pyrolysis. In this study, the electrostatic spinning solution is composed mainly of polyvinyl pyrrolidone, ethyl silicate (TEOS) and AgNO$_3$. The structural and morphological studies of the materials after calcination were investigated using X-ray diffraction, scanning electron microscopy, transmission electron microscopy (TEM) and thermogravimetric analysis–differential scanning calorimetry (TG–DSC). The results indicated that the samples had a rough surface structure. The load on the nanofibers was silver (Ag) metal, and the number and grain size of Ag nanoparticles increased as the relative amounts of AgNO$_3$ increased. Furthermore, the surface enhanced Raman scattering (SERS) activity of the Ag/SiO$_2$ was investigated using the common antibiotic enrofloxacin as a probe. It was found that the amorphous silica fiber with uniform loading of Ag nanoparticles exhibited a strong SERS enhancement effect. Due to the analytical performance, the predicted potential for SERS detection of trace antibiotics is excellent.

✉ Zhigang Chen
czg@mail.usts.edu.cn

[1] School of Chemistry, Biology and Materials Engineering, Suzhou University of Science and Technology, Suzhou 215009, China

[2] Jiangsu Key Laboratory for Environment Functional Materials, Suzhou University of Science and Technology, Suzhou 215009, China

1 Introduction

Antibiotics have made tremendous contributions to human health. Unfortunately, the overuse of antibiotics has also resulted in negative impacts as well. These include environmental toxicity several side effects on the human body such as the destruction of normal bacteria within the human body, weakened efficacy of the antibiotics, and so on. For these reasons, among others, detecting the presence of trace amounts of antibiotic residues has become a strong area of focus for many researchers [1]. At present, the commonly used method for detecting trace antibiotics is chromatography [2]. Although the results of this traditional detection method are accurate, it is a costly and time consuming method that requires a lot of preparation.

The SERS effect can reveal structural information about the tested material at the molecular level [3]. With the continuous development of nanomaterials, using SERS for detecting trace amounts of harmful substances existing in the environment has attracted widespread attention [4]. Raman spectroscopy results in no damage, requires no pretreatment of the sample, and is suitable for quick, easy analysis of liquid samples. Preparing the repeatable and uniform active substrate with an appropriate enhancing activity is the key to determining the trace amount and to quantitative detection. At present, the research on this kind of basement has mainly focused on the silver substrate [5, 6]. This is because the materials with desirable characteristics are currently found only in the nano structure of gold, silver, copper and some transition metals, and nano silver is not only cheap but also has a higher enhancement effect in the visible light range than other materials. Several preparation methods have been used, including electrochemical methods [7], biological methods [8], chemical deposition [9] and the sol–gel method among others. The most commonly used method is

chemical reduction [10], which has the ability to manipulate the size of colloidal particles through proper selection of initial concentrations of the substrates. However, this method is inevitably effected by impure ions. Acosta and co-workers synthesized silver nanorods with a diameter of 150 nm using silver nitrate as the silver source, adding ethylene glycol and PVP as the stabilizer [11]. This method however has the disadvantage of a lengthy reaction time.

In this paper, we report a simple and effective method for the synthesis of nano silver substrate. The proposed method uses the materials-processing technique of electrospinning, which provides a viable approach for the fabrication of fibers with diameters ranging from nanometers to microns [12]. Therefore, the incorporation of Ag nanoparticles in the silica fiber not only provides a stable carrier for the Ag nanoparticles, but also improves the performance and stability of these nanoparticles. More importantly, it can be shown that this membrane material shows good SERS activity as a substrate for ENR [13, 14], which is a commonly used antibiotic that has the possibility of leaving residues in animals and plants. The experimental limits of detection were 10 nmol/L. These results show that such a substrate has a very high sensitivity and application value, and has the potential to be used for the detection of trace amounts of antibiotics.

2 Experimental

2.1 Materials

PVP (Mw = 1,300,000), $AgNO_3$ (the precursor of in-situ synthesized Ag), ethyl silicate (TEOS) and analytical grade ethanol were purchased from the Sinopharm Chemical Reagent Co., Ltd.

2.2 Preparation of Samples

First, 2.00 g polyvinyl pyrrolidone (PVP) was dissolved in 30 ml ethanol, and stirred for 3 h at room temperature. Then, 4.46 mL ethyl silicate (TEOS) was added to the above solution, followed by stirring for 6 h. Next, 0.085 g Ag $(NO)_3$ was added into 5 mL ultrapure water, and after stirring for 20 min, the resulting solution was mixed with the PVP/TEOS composite and stirred for 2 h to prepare a PVP/TEOS/Ag $(NO)_3$ composite. A light brown homogeneous and viscous solution resulted and was subsequently used for electrospinning.

The composite solution was then loaded into a 5 ml plastic syringe, with an internal pinhead diameter of 0.5 mm. The pinhead was connected to a high voltage supply which was capable of generating direct current voltages of up to 30 kV. In the experiment, a voltage of 16 kV was applied for electrospinning. A fiber collector of electrically grounded

aluminum foil that covered a metal plate served as the counter electrode, and the distance between the tip of spinneret and the collector was 20 cm. The flow rate of the solution was maintained at 0.5 mL/min. The relative humidity of the external environment was maintained below 50%.

After the spinning process, the as-electrospun composite nanofibers were placed in a vacuum oven for 6 h at 30 °C in order to remove the solvent residuals. In order to remove the PVP completely, the composite nanofibers were calcinated in air at 600 °C for 4 h. Via this process, Ag-doped SiO_2 nanofibers were obtained.

The specific experimental details for Raman spectroscopy are as follows. Enrofloxacin (ENR) was dissolved in ethanol to obtain a specific solution concentration. The solution was then rapidly dripped onto the prepared material and then tested using Raman spectra.

2.3 Characterization

The surface morphology and microstructure of the samples were characterized using field emission scanning electron microscopy (FESEM; Hitachi S-4800). To characterize the crystal structure and elemental analysis of the nanofiber specimens, X-ray diffraction (XRD; CuKα, λ ¼1.5406 Å) and transmission electron microscopy (TEM; FEI Tecnai F30) were employed respectively. The materials were characterized by Raman microscopy using a DXR Raman Microscope confocal laser produced by Thermo Fisher Scientific.

3 Results and Discussion

3.1 Thermogravimetric and Microstructure Analysis

Thermogravimetric analysis–differential scanning calorimetry results of the as-spun composite nanofibers PVP/TEOS/Ag(NO)_3 are shown in Fig. 1a. According to the TG–DSC results, the organic materials were completely decomposed before reaching around 600 °C, and the inorganic materials remained around 25 wt% from the specimens of nanofibers. The initial weight loss in the TG curve could result from the loss of the surface-adsorbed solvent or the residual solvent molecules in the composite fibers. Part of the decomposition process of the PVP took place between 100 and 300 °C through a slow process of weight loss. Concurrently to this, the system is undergoing an endothermic process and there were two sharp exothermic peaks. The reduction of silver nitrate and the complete decomposition of PVP occurred at 382 °C. TEOS reacted with oxygen in the air to form silicon dioxide at 425 °C. The result of the calcination was Ag-doped SiO_2 nanofibers. XRD patterns were employed to identify the phase composition and crystal structure of the Ag-doped SiO_2 nanofibers (Fig. 1b). The diffraction peaks
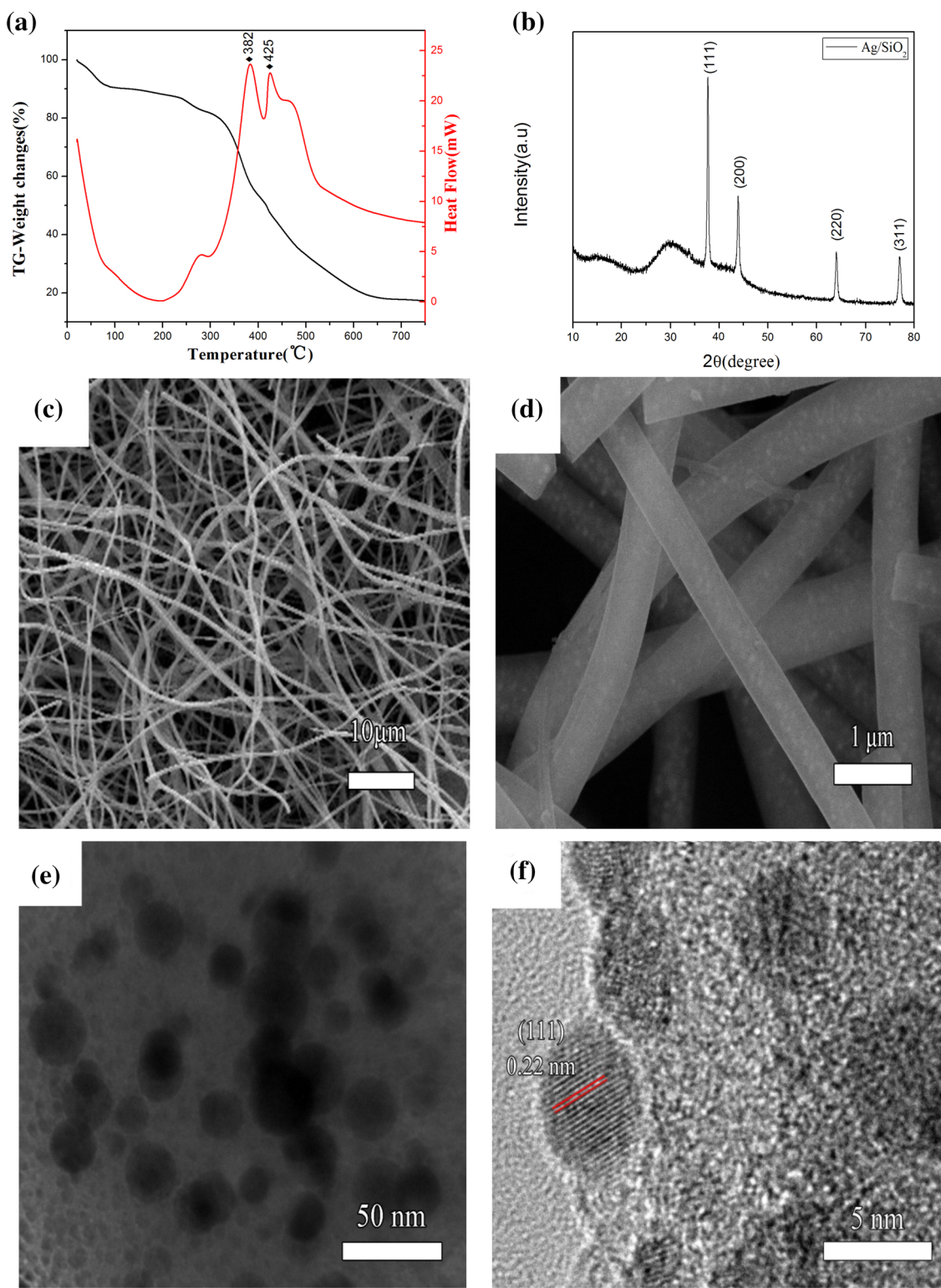
Fig. 1 a TG-DSC curves of PVP/TEOS/Ag (NO)$_3$ fibers in air, **b** XRD of Ag/SiO$_2$ fibers pyrolyzed at 600 °C, **c, d** SEM images at different resolution; the scale bars are 1 μm and the scale bars in the enlarged views are 250 nm, **e, f** are TEM and HRTEM images of Ag/SiO$_2$ fibers, respectively

at $2\theta = 37.98°$, $44.18°$, $64.42°$ and $77.26°$ were assigned to the corresponding diffraction signals (111), (200), (220) and (311), which indicated the cubic crystal structure of Ag (JCPDS Card No.04-0783). There was a steamed bread diffraction peak around 30°, which corresponds to the amorphous silica. The microstructures of the samples were investigated through analysis of SEM images. As shown in Fig. 1c, the product is made up of a number of non-agglomerate and disordered fibers. This causes it to have a rough surface structure. A substantial number of nanofibers with diameters ranging from 500 to 800 nm and lengths of several tens of micrometers can be observed in the Fig. 1d. It can be clearly seen that the nanofibers consist of amorphous silica and Ag nanoparticles. Ag nanoparticles are uniformly distributed on the surface and inside of the SiO_2. Further morphology characterization of the product was carried out using TEM (Fig. 1e), and the results were consistent with the FE-SEM results. There are several spherical silver particles with a particle diameter of about 30 nm. More interestingly, the spatial distribution of Ag nanoparticles results in shadow overlaps. The HRTEM image of the Ag nanoparticles assembled on the fibers (Fig. 1f) displays clear Ag lattice fringes with interplanar distance equivalents of 0.22 nm corresponding to a (1 1 1) plane, and the Ag/SiO_2 nanofibers are polycrystalline in structure.

3.2 Scanning Electron Microscope Analysis

By controlling the different $AgNO_3$/TEOS molar ratios: 1:40 (Fig. 2a), 1:20 (Fig. 2b), and 1:10 (Fig. 2c); we can see clearly that the average diameter of the nanoparticles was about 30, 40, 60 nm, respectively. So, the number and particle size of Ag nanoparticles increases as the relative amounts of $AgNO_3$ increased, which can be attributed to the fact an increase in silver strengthens the aggregation of silver particles.

3.3 XPS Analysis

In order to further determine the properties of silver in materials, XPS tests were carried out on the materials. Figure 3a is the XPS spectrum of the material. Figure 3b is the Ag3d spectrum. As can be seen from the graph, the peak at the 368.1 corresponded to the silver elements. This also indicated that a large number of silver elements exist inside the material.

3.4 Raman Analysis

Raman spectra of the samples were conducted to investigate the SERS activity of Ag nanoparticles supported on silica
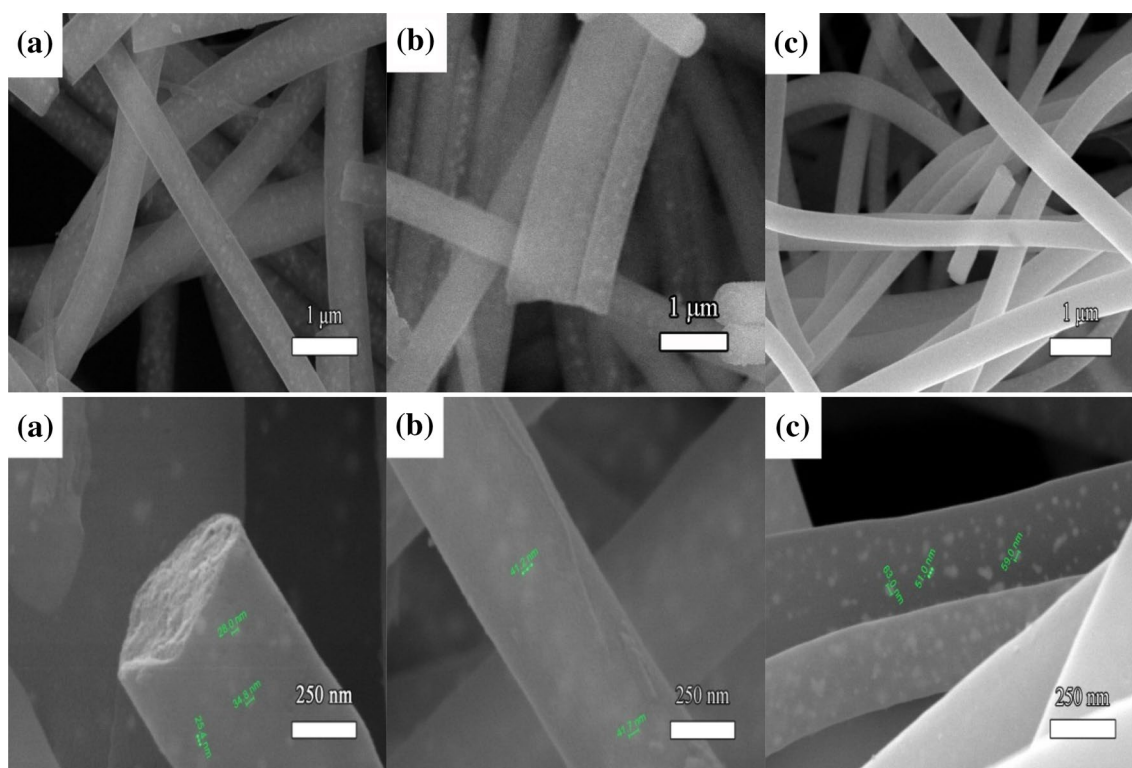

Fig. 2 SEM micrographs of Ag/SiO_2 with different $AgNO_3$/TEOS molar ratios: **a** 1:40, **b** 1:20 and **c** 1:10; scale bars are 1 μm, and the scale bars in the enlarged views are 250 nm
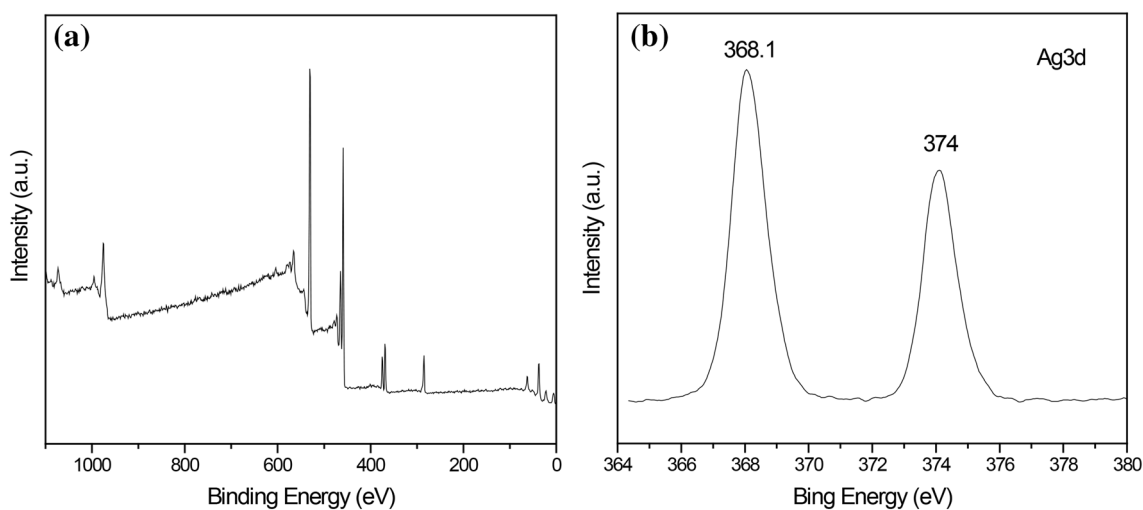
Fig. 3 XPS spectra of materials

fiber membrane materials; the results are shown in Fig. 4a. Naturally, there are no Raman signals from Ag/SiO$_2$. If this membrane is used as the surface-enhanced Raman substrate material, it can eliminate its own Raman signal, making it a very suitable Raman substrate material. We explored the potential of Ag/SiO$_2$ for SERS applications by taking enrofloxacin (ENR), a common antibiotic, as the research object. The Raman spectrum shown in Fig. 4b is a 1×10^{-4} mol/L ENR solution. A series of characteristic peaks of ENR were observed between 500 and 2000 cm^{-1}. As can be seen, the intensity of the peaks is very low. However, when the ENR solution was dripped onto the film containing Ag nanoparticles, we were surprised to find that the Raman intensity was greatly enhanced. As shown in the Fig. 4c, all the characteristic peaks of ENR are vastly enhanced, especially the main characteristic peaks of ENR [15]. The Raman band at 1390 cm^{-1} is the most intense, which corresponds to the symmetric stretching vibration of O–C–O. The benzene ring vibration and stretching peaks are at 1476 and 1550 cm^{-1}, respectively. The characteristic peak of 1620 cm^{-1} corresponds with the O–C stretching vibration. The above phenomenon fully demonstrates that the membrane loaded with Ag nanoparticles has a very strong surface-enhanced Raman ability, where both electromagnetic enhancement and chemical enhancement [16] contribute to the total SERS enhancement. The first contributing factor that enhanced the Raman base material was the rough surface. The surface consisted of a homogeneous distribution of Ag nanoparticles, constituting a spatial stereo structure. When the incident laser excites the Ag nanoparticles on the substrate, it can lead to collective oscillation of both the particle and metal surface free electrons. In this case, the incident photon couples with the matching nano metal structure of the free electron, resulting in local surface plasmon resonance [17]. Thereby

forming a more intense electromagnetic field in this space. Raman scattering is accompanied by a two-photon process, which greatly improves the Raman signal intensity of the adsorbed molecule. Simultaneously, the chemical interaction between Ag nanoparticles and ENR molecules further improves the molecular polarization. This improvement is attributed to the chemical enhancement from the charge transfer between adsorbed Ag molecules and ENR. Therefore, further enhancing the Raman intensity.

For Ag nanoparticle materials with different particle diameters (Fig. 2), the enhanced Raman signal of ENR also differs. It can be seen from the Raman spectrum shown in Fig. 4d that Raman enhancement for ENR is very intense and the characteristic peaks are consistent. However, the substrates with smaller particle sizes have an even greater intensity.

In order to research the detection limit of this SERS substrate material on an ENR solution, the concentrations were measured from 1×10^{-4} to 1×10^{-8} mol/L, shown in the Fig. 4f. It is clear from these results that the intensity of the Raman characteristic peak gradually decreases as the concentration of the ENR solution decreases. When the concentration is 1×10^{-7} mol/L, the main characteristic peak is still very clear. At the concentration of 10 nmol/L, there is still one characteristic peak present at 1390 cm^{-1}. Therefore, the experimental limits of detection were 10 nmol/L, thus fully demonstrating the great potential of using the substrate material in the detection of traces of ENR.

3.5 Mechanism Diagram of SERS

In Fig. 5, the mechanism of SERS is clearly visualized. It is widely accepted that the Raman enhancement is attributed to the change of the electric field and the molecular
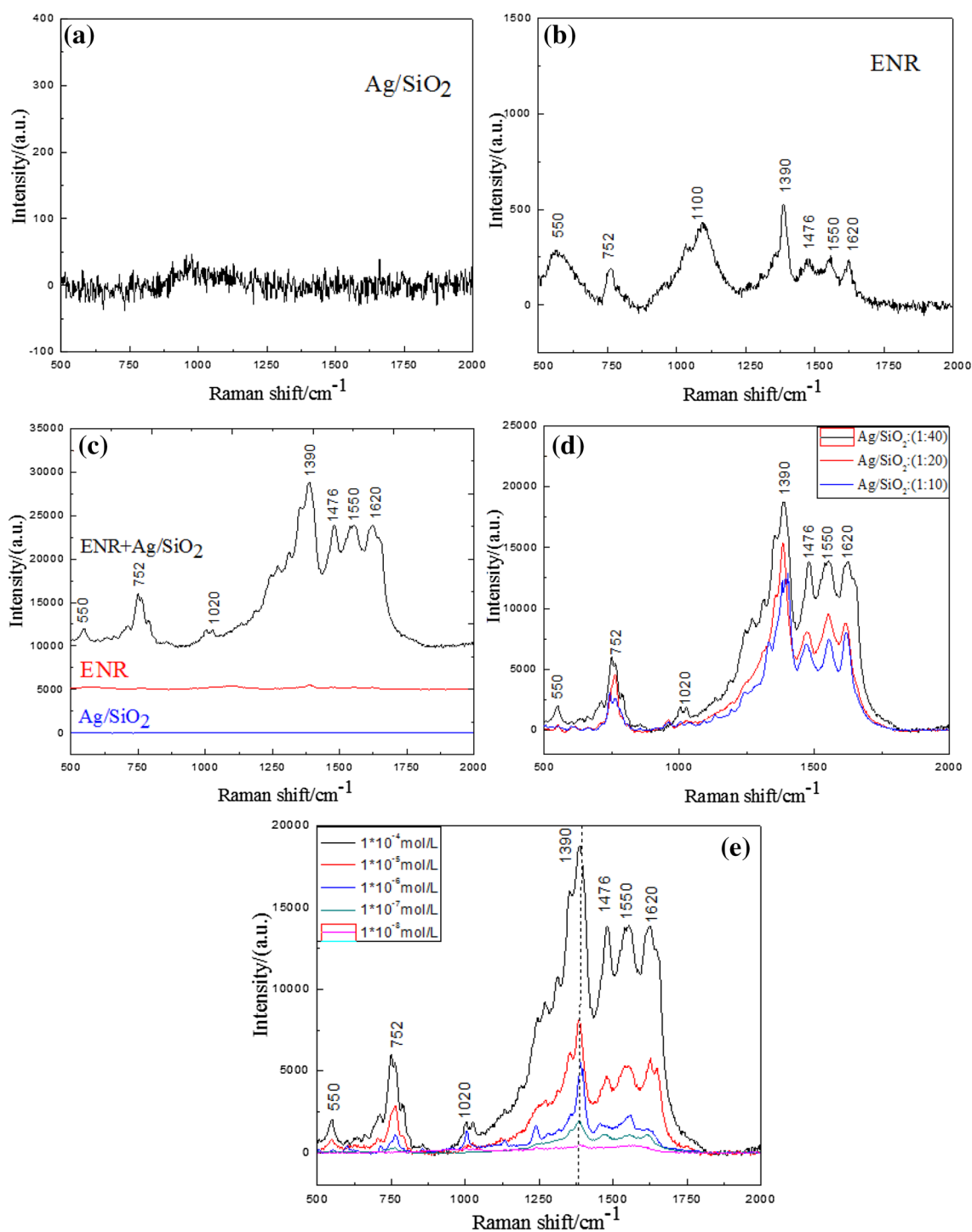
Fig. 4 The Raman spectra of **a** Ag/SiO$_2$, **b** ENR solution (1×10^{-4} mol/L), SERS spectra of **c** ENR solution (1×10^{-4} mol/L) dropped on Ag/SiO$_2$ fiber membrane, **d** Ag/SiO$_2$ with different AgNO$_3$/TEOS molar ratios, and **e** different concentration of ENR solution

polarization. The Raman substrate material had a rough surface, and the Ag nanoparticles constituted a spatial stereo structure. When the incident laser excited the Ag nanoparticles, it led to collective oscillation of both the particle and metal surface free electrons. In this case, the local surface

plasmon resonance was caused by incident photon couples with the matching nano metal structure of the free electron, thereby forming a more intense electromagnetic field in this space. Raman scattering was accompanied by a two-photon process, which greatly improved the Raman signal intensity
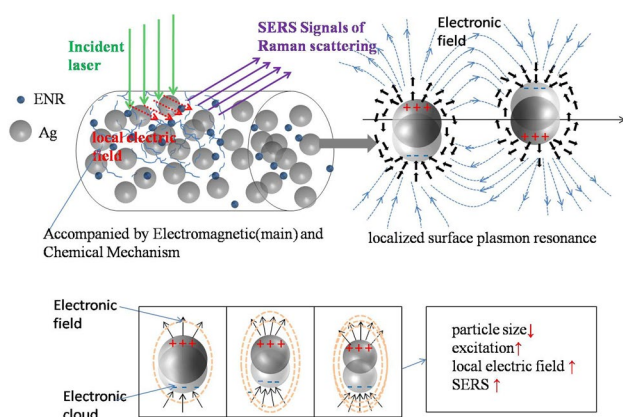
Fig. 5 Mechanism diagram of SERS

of the adsorbed molecule. At the same time, the chemical interaction between Ag nanoparticles and ENR molecules also improved the molecular polarization. Therefore, the Raman intensity was further enhanced. The lower part of the Mechanism diagram for SERS explains the phenomena in Fig. 4c. Because smaller Ag particles were more easily excited by the incident light, this caused a local surface plasmon resonance to be induced, which in turn had a stronger electromagnetic field.

4 Conclusion

Ag nanoparticles supported on SiO_2 fibers were synthesized using the electrospinning method. The surface structure of this film's materials and the distribution and particle size of the Ag nanoparticles were then comprehensively characterized, and investigated via the SERS effect using enrofloxacin as the subject. This research found the performance of the nanofiber material to have a high sensitivity, quick response, and good selectivity. The experimental limits of detection were 10 nmol/L. The results demonstrate that Ag-doped SiO_2 nanofibers have excellent potential applications in SERS detecting.

References

1. N. Kemper, Veterinary antibiotics in the aquatic and terrestrial environment. Ecol. Indic. **8**, 1–13 (2008)

2. Q. Xue, Y. Qi, F. Liu, Ultra-high performance liquid chromatography-electrospray tandem mass spectrometry for the analysis of antibiotic residues in environmental waters. Environ. Sci. Pollut. R **22**, 1–11 (2015)

3. S. Nie, S.R. Emory, Probing single molecules and single nanoparticles by surface-enhanced raman scattering. Science **275**, 1102–1106 (1997)

4. J.F. Betz, W.W. Yu, Y. Cheng, I.M. White, G.W. Rubloff, Simple SERS substrates: powerful, portable, and full of potential. Phys. Chem. Chem. Phys. **16**, 2224 (2014)

5. W. Liu, J. Lu, H. Xu, A. Patel, Z.S. Chen, Silver nanoparticles: Synthesis, properties,and therapeutic. Drug Discov. Today Silver **20**, 595–601 (2015)

6. L. Ge, Q. Li, M. Wang, J. Quyang, X. Li, M.M. Xing, Nanosilver particles in medical applications: synthesis, performance, and toxicity. Int. J. Nanomed. **9**, 2399–2407 (2014)

7. F.M. Reicha, A. Sarhan, M.I. Abdel-Hamid, I.M. Ei-Sherbiny, Preparation of silver nanoparticles in the presence of chitosan by electrochemical method. Carbohydr. Polym. **89**, 236–237 (2012)

8. K. Chaloupka, Y. Malam, A.M. Seifalian, Nanosilver as a new generation of nanoproduct in biomedical applications. Trends Biotechnol. **28**, 580–588 (2010)

9. H.H. Zhang, F. Zhou, M. Liu, D.L. Liu, D.D. Men, W.P. Cai, G.T. Duan, Y. Li, Spherical nanoparticle arrays with tunable nanogaps and their hydrophobicity enhanced rapid SERS detection by localized concentration of droplet evaporation. Adv. Mater. Interfaces **2**, 120–126 (2015)

10. J. Pulit, M. Banach, Z. Kowalski, Chemical reduction as the main method for obtaining nanosilver. J. Comput. Theor. Nanosci. **10**, 276–284 (2013)

11. A. Gomez-Acosta, A. Manzano-Ramirez, E.J. Lopez-Naranjo, Silver nanostructure dependence on the stirring-time in a high-yield polyol synthesis using a short-chain PVP. Mater. Lett. **138**, 167–170 (2015)

12. K. Castkova, K. Maca, J. Sekaninova, J. Nemcovsky, J. Cihlar, Electrospinning thermal treatment of yttria doped zirconia fibres. Ceram. Int. **43**, 7581–7587 (2017)

13. C. Li, J. Chen, J. Wang, Z. Ma, P. Han, Y. Luan, A. Lu, Occurrence of antibiotics in soils and manures from greenhouse vegetable production bases of Beijing, China and an associated risk assessment. Sci. Total Environ. **522**, 101–105 (2015)

14. F. Yu, S. Yu, L. Yu, Y. Wu, H. Zhang, L. Qu, P.B. Harrington, Determination of residual enrofloxacin in food samples by a sensitive method of chemiluminescence enzyme immunoassay. Food Chem. **149**, 71–75 (2014)

15. Y. Zhang, Y. Huang, F. Zhai, R. Du, Y. Liu, K. Lai, Analyses of enrofloxacin, furazolidone and malachite green in fish products with surface-enhanced Raman spectroscopy. Food Chem. **135**, 845–850 (2012)

16. H.Y. Guo, Z.Y. Zhang, B.S. Xing, A. Mukherjee, C. Musante, J.C. White, L.L. He, Analysis of silver nanoparticles in antimicrobial products using surface-enhanced raman spectroscopy (SERS). Environ. Sci. Technol. **49**, 4317–4324 (2015)

17. M. Kuisma, A. Sakko, T.P. Rossi, A.H. Larsen, J. Enkovaara, L. Lehtovaara, T.T. Rantala, Localized surface plasmon resonance in silver nanoparticles: Atomistic first-principles time-dependent density-functional theory calculations. Phys. Rev. B **91**, 115431 (2015)